

Ultra-Thin Graphene Oxide (GO)-DNA Composite Polymerization Gels (CPGs)

Ruohong Shi¹, Qi Huang¹, Rebecca Schulman^{1-4*}, and David H. Gracias^{1, 3-8*}

¹Department of Chemical and Biomolecular Engineering, Johns Hopkins University, Baltimore, MD, USA.

²Department of Computer Science, Johns Hopkins University, Baltimore, MD, USA.

³Laboratory for Computational Sensing and Robotics (LCSR), Johns Hopkins University, Baltimore, MD, USA.

⁴Department of Chemistry, Johns Hopkins University, Baltimore, MD, USA.

⁵Center for MicroPhysiological Systems (MPS), Johns Hopkins University, Baltimore, MD, USA.

⁶Department of Oncology, Johns Hopkins School of Medicine, Baltimore, MD, USA.

⁷Sidney Kimmel Comprehensive Cancer Center (SKCCC), Johns Hopkins School of Medicine, Baltimore. MD. USA.

⁸Department of Materials Science and Engineering, Johns Hopkins University, Baltimore, MD, USA.

*Corresponding authors: dgracias@jhu.edu; rschulman@jhu.edu

DNA polymerization gels are a new class of soft programmable materials capable of reversible 100-fold volumetric size changes induced by DNA-specific strand displacement reactions. By incorporating DNA circuits and spatial patterns, these gels could orchestrate complex, self-regulating processes of relevance to biosensing, robotics, and medicine. However, the ultrasoft nature of the gels and slow response times can limit applicability. We developed GO-DNA composite polymerization gels (CPGs) by blending DNA gels with graphene oxide (GO). Photopatterned ultra-thin GO-DNA CPG films, as thin as 8 µm, were achieved. Notably, GO-DNA CPGs exhibited similar rates of swelling but 60 times faster shrinking, suggesting that the introduction of inorganic nanoparticles could provide a means to tune the mechanical properties and swelling characteristics of DNA polymerization gels.

INTRODUCTION

Motivated by applications in biosensing, soft robotics, and medicine, in recent years there has been a growing interest in the development of stimuli-responsive hydrogels capable of undergoing substantial changes in volume when exposed to various environmental stimuli, including pH, light, and temperature. [1,2] Biomolecular stimuli-responsive materials, such as gels that respond to enzymes, antibodies, and nucleic acids, are especially appealing for biosensing, biomedical, and bioinspired applications. [3]

Due to DNA's reproducible and programmable base pairing, DNA-based hydrogels have emerged as an important class of biomaterials. [4-7] These hydrogels have been engineered to respond to various stimuli, including temperature, ions, and small molecules. We previously reported a DNA-crosslinked polyacrylamide hydrogel, also known as DNA polymerization hydrogel, since it swells by sequentially introducing multiple DNA hairpins. Compared to other DNA gels, which show limited swelling, these polymerization hydrogels expand up to 100-fold. [8] There have been several advances in tuning the structure and properties of these gels, such as varying the polymer backbone to tune the stiffness and biocompatibility. [9] Along with synthesis, photopatterning protocols have also enabled the fabrication of CAD-designed shapes with high spatial resolution. [8-10] Further, we devised a mechanism for reversible shape change, employing one set of DNA triggers for swelling and another for shrinking. We have utilized this scheme to create gel automata. [10]

To broaden the applicability of DNA gels, approaches must be developed to modulate the mechanical network of the gels. [11] We previously observed that Am-co-DNA and gelatin-based gels exhibited low shear moduli, approximately 500 and 300 Pa, respectively. [9] In prior studies, we varied the concentration of the chemical crosslinker, Bis-acrylamide, within Am-based DNA gels. Increasing the concentration of Bis-acrylamide covalent crosslinks enhanced the gels' shear modulus. Still, there was a trade-off in that the increased crosslink density resulted in a decreased swelling ratio. Specifically, when compared with pure Am-DNA gels, Am-BIS-DNA gels with 10 mM BIS-Am crosslinkers displayed a roughly four times higher shear modulus, but their swelling ratio was reduced to one-fifth. We could also tune the modulus of the gels by altering another parameter, the molecular weight (MW) of the PEGDA macromer in PEG-co-DNA hydrogels. We observed that reducing the MW of PEGDA from 20k to 575 led to PEG-co-DNA gels virtually incapable of DNA-directed swelling. These two results suggest an inherent trade-off between the swelling capacity and the stiffness of the material. In pursuit of a compromise between these two properties, we selected PEG10k and Am-5mM BIS

gels, which offered a balance of relatively high toughness and substantial swelling in recent investigations. We wondered whether DNA polymerization gels' mechanical properties could be further enhanced without compromising their programmability, particularly for applications like robotics.

Furthermore, gaining a deeper understanding of the kinetics of DNA polymerization gel actuation can enhance our ability to modulate their performance. We observed that DNA-directed swelling tends to reach a plateau within 1-3 days; the DNA-directed shrinking process is relatively faster, albeit still taking several hours to complete. ^[10] Previously, we explored the possibility of modulating the swelling response of DNA polymerization gels by varying parameters such as the design and concentration of DNA crosslinks within the hydrogels, the structure of DNA hairpin triggers, and the ionic strength of the solution in which the swelling occurs. Tuning these variables can alter the swelling rate and extent but only marginally. ^[9]

The dimensions of a material critically influence the time required for the transport of the components such as DNA molecules, ions, and water throughout the material. As a result, transport processes are likely to be important for understanding the time needed to swell or shrink DNA polymerization gels. As a first-pass approximation, the Stokes-Einstein equation indicates that the diffusion rate is inversely proportional to the material's dimensions. [12] Hence, we hypothesized that a reduction in the thickness of the DNA gel should lead to accelerated swelling, as the characteristic time for diffusion should decrease. Indeed, researchers have previously observed that thinner structures bend more rapidly. [8,13,14] However, patterning free-standing, ultra-thin (< 60 microns) DNA polymerization gels is a big challenge due to their ultrasoft nature, which results in breakage during their release from the substrate. This rupture is a problem of broad relevance to all ultrathin photopatterned gels, and the propensity for breakage increases as the lateral dimensions of the patterns increase. In our prior studies, the smallest dimensions achieved through photopatterning were 1 mm \times 1 mm gel sheets with a thickness ranging from 60 to 70 μ m.

Apart from blending with organic copolymers and monomers, the inclusion of inorganic nanoparticles into hydrogel polymeric networks is an alternate approach for modifying the mechanical, swelling properties and functionality of hydrogels. [15-21] Among these, graphene and related 2D layered materials (2DLMs) have emerged as promising filler materials. [22-25] Graphene hydrogel composites have been developed and applied for energy storage, wastewater treatment, biosensors, and biomedicine. Notably, graphene oxide (GO) has gained significant attention in recent research due to its good hydrophilicity, attributed to polar groups that allow for uniform dispersion in solvents. The incorporation of GO into polymer composites results in the formation of crosslinking between GO polar groups and polymeric branches, significantly enhancing the mechanical performance of the resulting composite materials. [26-29]

This work studies the effects of incorporating GO nanosheets into AM-BIS and PEG-based DNA polymerization gels. We characterize their swelling and shrinking behavior across a range of thicknesses.

RESULTS & DISCUSSION

The GO-DNA CPG synthesis involves multiple components, including GO nanosheets, a base polymer (Am-BIS or PEG), and acrydite-modifed DNA-crosslinks (Fig. 1). The photopatterned gel has both chemical and physical crosslinks and can be swollen or shrunk with DNA hairpins. In this work, we synthesized and photopatterned (a) PEG-co-DNA/GO CPGs in 1 mm \times 1 mm squares, with thicknesses of 160 μm , 16 μm , and 8 μm and (b) PAAM-co-BIS-DNA/GO gels with thicknesses of 160 μm and 16 μm . Attempts

were made to produce PAAM-co-BIS-DNA/GO gels with thicknesses below 10 μ m. However, these gels adhered to the glass substrate and broke during release from the underlying substrate, and further studies with alternate sacrificial layers (such as polyacrylic acid (PAA)) may enable photopatterning and release of even thinner PAAM-co-BIS-DNA/GO CPGs. After photopatterning the gels into square-shaped sheets, we examined their physical appearance and DNA-directed swelling/shrinking behavior. We observed that the gels displayed interesting mechanical, optical, and swelling properties, as detailed in the subsequent sections.

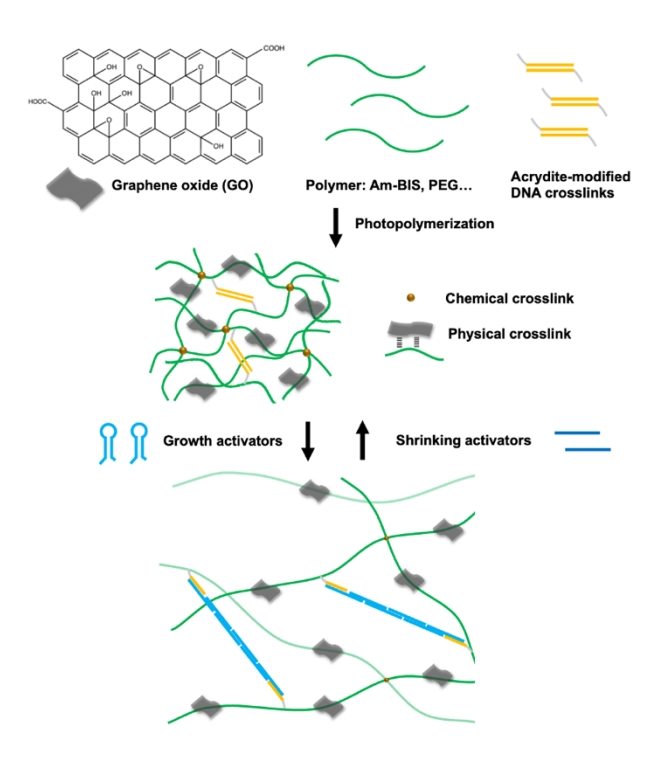


Figure 1. Schematic of the molecular components and swelling/shrinkage of GO-DNA CPGs. Sequential insertion of hairpin-shaped growth activators drives polymerization at acrydite-modified DNA crosslinks, and thus, the growth of DNA gels. The shrinking activators drive depolymerization at acrydite-modified DNA crosslinks, and thus, DNA gel shrinking. [10]

We first fabricated GO/PEG-co-DNA CPGs with similar thickness (160 $\mu m)$ to prior work (Figure 2a). These as-fabricated GO-DNA CPGs displayed a light-yellow hue with black speckles due to the incorporation of GO. While the GO appeared uniformly dispersed throughout the gel, some aggregation was observed. The gels exhibited clean, sharp edges and straight sides, suggesting they could be photopatterned with good fidelity (Figure 2b). Subsequently, we fabricated much thinner (16 $\mu m)$ GO/PEG-co-DNA CPGs. Notably, these thinner gels were significantly more transparent than their 160 μm counterparts and appeared more flexible with curved corners in the buffer solution (Figure 2c).

Upon adding methacryloxyethyl thiocarbamoyl rhodamine B fluorescent dye, the 160 μm thick GO/PEG-co-DNA CPGs transformed into a vibrant magenta color when contrasted against a dark background (Figure 2d). Notably, the thinner gels (16 μm and 8 μm) with the same dye retained visibility to the naked eye, facilitating easy handling (Figure 2e and 2f). The 8 μm thick GO/PEG-co-DNA CPGs were similarly flexible and tended to float on the surface of the TAEM buffer solution. A pipette was used to deposit additional solution atop the 8 μm gels to ensure full submersion for subsequent actuation experiments.

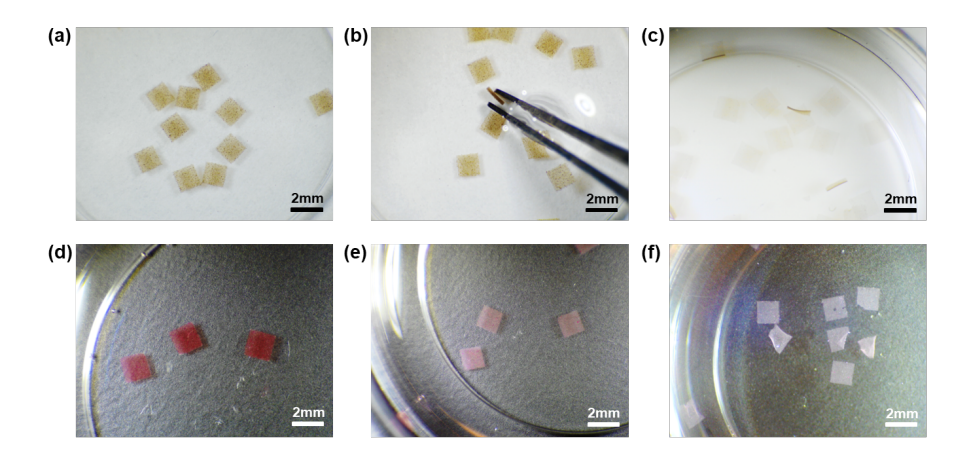


Figure 2 | Bright-field images of GO-DNA CPGs. (a) Top view of 160 μ m thick photopatterned GO/PEG-co-DNA CPGs. (b) Top and side view (in the grip of a tweezer) of photopatterned GO/PEG-co-DNA CPGs. (c) Top and side view of 16 μ m thick GO/PEG-co-DNA CPGs. Top view of (d) 160 μ m thick, (e) 16 μ m thick, and (f) 8 μ m thick GO/PEG-co-DNA CPGs dyed with Rhodamine.

DNA-directed Swelling Process

Our first objective was to ascertain if the DNA activators, which are effective for non-composite DNA polymerization gels, retain their functionality upon adding GO. We fabricated 160 μ m thick PEG-co-DNA gels and verified the approximately 0.6-fold change in side length in approximately 100 hours on the addition of growth activators (60 μ M of System III growth activators with 1% growth terminators, see Table S1), consistent with previously reported values (Figure S1a). Subsequently, we applied the same activator conditions to GO/PEG-co-DNA CPGs, which exhibited a comparable degree of swelling (Figure S1b). As a control, we also monitored gels soaked in TAEM buffer for 100 hours; no significant shape change was observed (Figure S1c). These results indicate that GO/PEG-co-DNA CPGs maintain a similar capacity for swelling in the presence of DNA growth activators, and the electrostatic interactions of DNA with GO do not impede swelling.

Then, we systematically characterized the swelling of GO-DNA CPGs with time intervals of 30 minutes and measured the side lengths of the gels using MATLAB (Figure 3, Figure S2). The relative change in side length ($\Delta L/L_0$) of the gel was calculated using the measured side lengths (L) from each image in a time series relative to the side length prior to adding DNA activators (L_0). In Figure 3a, we observed that the GO/PEG-co-DNA CPG sheets with thicknesses of 160 µm, 16 µm, and 8 µm have a final degree of swelling ($\Delta L/L_0$) of 0.6, 0.4, and 0.6, respectively. The swelling rates of the first 20 hours for all three thicknesses are largely the same, and the swelling also plateaus at around 50 hours, like non-composite PEG-co-DNA gels. The observation of no significant difference in swelling rate with GO/PEG-co-DNA CPGs of different thicknesses suggests that the swelling is not rate limited by diffusion but rather by DNA binding rates.

With GO/PAAM-co-BIS-DNA CPGs, we observed that the thinner 16 μm gels have a higher initial rate in the first 5 hours and plateau at a final degree of swelling ($\Delta L/L_0$) of 0.8 at around 10 hours (Figure 3b). The 160 μm gels plateau at a final degree of swelling ($\Delta L/L_0$) of 1.0 at around 25 hours. Non-composite PAAM-co-BIS-DNA gels with 160 μm thickness reached a similar final $\Delta L/L_0$ at around 40 hours. We note that the 16 μm thick GO/PEG-co-DNA CPG sheets can reach a swelling of 0.4 within 2 hours, which is a reasonable swelling extent and time scale for hydrogels used in present day untethered soft robots.

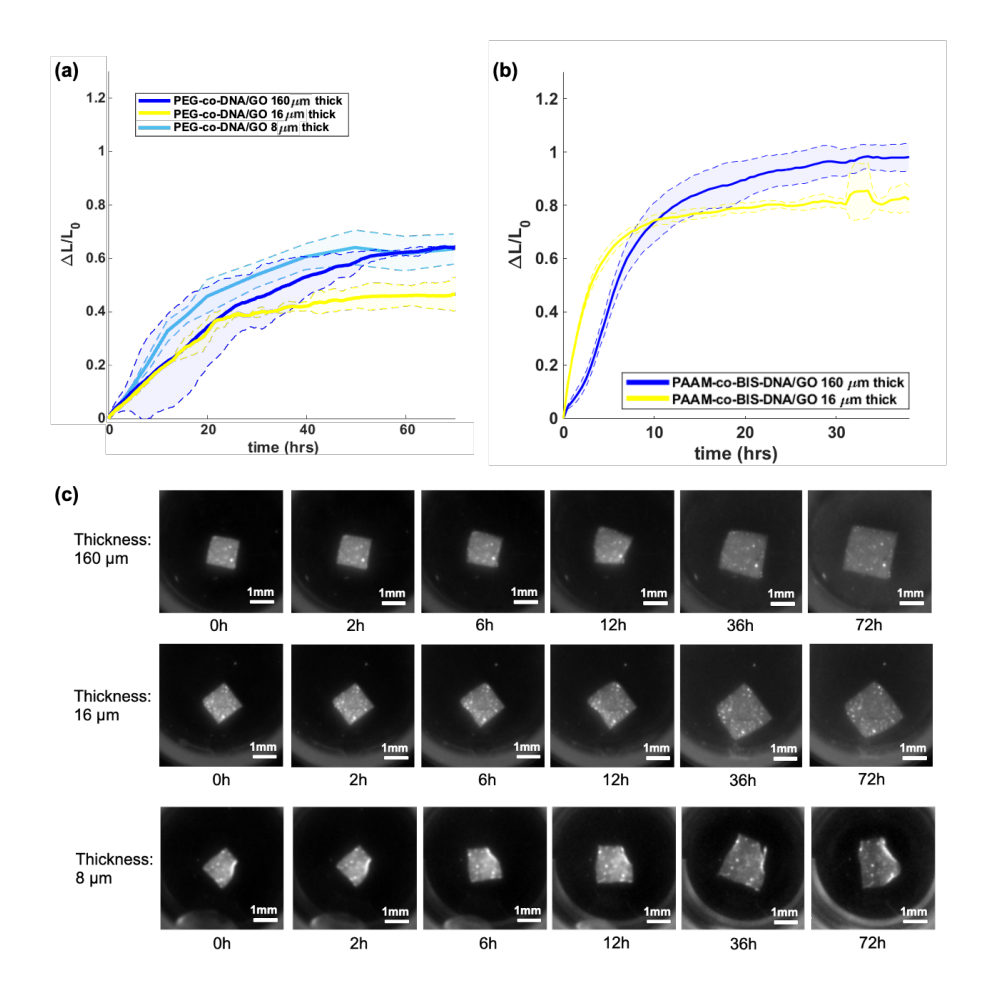


Figure 3 | Swelling characterizations of GO-DNA CPGs. (a) Swelling characterizations of GO/PEG-co-DNA CPGs with thicknesses of 160 μm, 16 μm, and 8 μm. (b) Swelling characterizations of GO/PAAM-co-BIS-DNA CPGs with thicknesses of 160 μm and 16 μm. The solid lines represent the relative change in side length (Δ L/L₀) of the gel, which was calculated using the measured side lengths (L) from each image in a time series relative to the side length before adding DNA activators (L₀). Shaded area/dotted lines enclose the standard deviation about the mean curvature value (N = 3). (c) Fluorescent micrographs of GO/PEG-co-DNA CPGs with varying thicknesses of 160 μm, 16 μm, and 8 μm swelling using DNA growth activators.

DNA-directed Shrinking Process

The swelling and shrinking dynamics in responsive hydrogels can vary due to factors like polymer affinity to water and reaction kinetics. In our previous studies, where we characterized the swelling and shrinking behavior of DNA polymerization gels, a difference in the rates was observed; shrinking plateaued within 5 - 8 hours, while swelling took considerably longer, plateauing after 1 - 3 days. We attribute this difference to the mechanistic and kinetic differences in DNA strand displacement during swelling and shrinking. Specifically, swelling involves the sequential insertion of DNA growth activators into DNA duplexes via a four-way branch migration, fostering the growth of the DNA polymer. Conversely, in the shrinking process, the activators bind to and simultaneously denature the DNA polymers.

During the shrinking phase of GO-DNA CPGs (Figure 4, Figure S3), we observed a markedly faster shrinking rate in both GO/PEG-co-DNA and GO/PAAM-co-BIS-DNA gels with a thickness of 160 μ m. Both the gel types reached steady states within 45 minutes, in contrast to the typical 5 hours observed in non-composite gels. We posit that this increased rate is attributable to a highly porous structure resulting from the addition of GO. Unlike the swelling process, shrinking rates displayed a strong correlation with gel thickness, suggesting that the shrinking process is diffusion-limited. Notably, the GO/PEG-co-DNA gels with an 8 μ m thickness exhibited near-instantaneous shrinking upon the addition of shrinking activators, reaching a steady state in just 6 minutes. Similarly, GO/PAAM-co-BIS-DNA gels with a 16 μ m thickness stabilized after only 8 minutes. Further studies are needed to investigate these observations in greater detail.

Throughout the intermediate stages of the shrinking process, we discerned a pattern of denser edges and a hollow center, as illustrated in Figure 4c (16 μm) at 30 minutes and Figure S3b at 5 minutes. This observation indicates that the accelerated shrinking process in thinner gels is anisotropic, initiating from the outer layers and progressively moving inwards towards the center. We previously observed similar anisotropic deformation with Am-DNA gel particles with a 1 mm diameter during swelling.

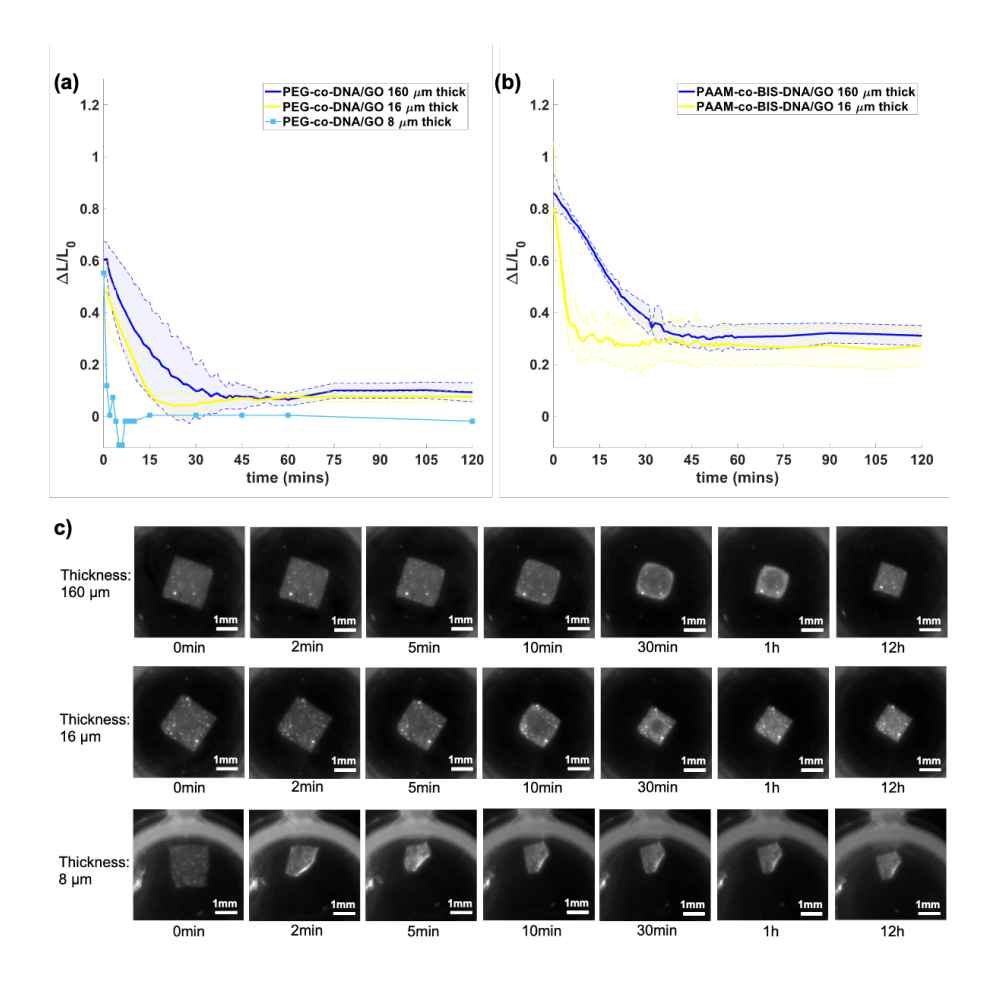


Figure 4 | Shrinking characteristics of GO-DNA CPGs. (a) Plot showing the extent of shrinkage of GO/PEG-co-DNA CPGs with thicknesses of 160 μ m, 16 μ m, and 8 μ m. (b) Plot showing the extent of shrinkage of GO/PAAM-co-BIS-DNA CPGs with thicknesses of 160 μ m and 16 μ m. The solid lines represent the relative change in side length ($\Delta L/L_0$) of the gel, which was calculated using the measured side lengths (L) from each image in a time series relative to the side length prior to adding DNA activators (L_0). Shaded area/dotted lines enclose the standard deviation about the mean curvature value (N = 3, except for GO/PEG-co-DNA CPGs at 8 μ m, where N = 1). (c) Time-lapse fluorescent micrographs of GO/PEG-co-DNA gels with varying thicknesses of 160 μ m, 16 μ m, and 8 μ m shrinking in size when exposed to DNA shrinking activators.

CONCLUSION

The development of ultra-thin GO-DNA CPGs, as presented in this study, expands the capabilities of programmable and mechanically robust soft materials. Our study demonstrates that incorporating GO into DNA polymerization gels substantially enhances the mechanical properties without compromising the gel's inherent responsiveness to DNA triggers. Furthermore, our findings reveal an acceleration in the shrinking kinetics of the CPGs, which is a significant stride toward their practical application in real-world settings, especially of relevance to soft robotics. The everexpanding research on GO continues to uncover new possibilities and applications in fields such as sensors, 3D printing, and beyond. Hence, the integration of GO into DNA polymerization gels represents a pivotal advancement in programmable soft materials.

This work also presented the relationships between materials dimension and actuation kinetics. These relationships can contribute to the construction of physical models, which can serve as invaluable tools in elucidating the intricate mechanical dynamics underlying the actuation process. This enhanced understanding can be harnessed to refine and optimize the material design strategy, paving the way to realize cutting-edge, high-performance programmable materials.

Future efforts in GO-DNA CPGs should encompass a comprehensive and detailed approach to structural characterization and mechanical performance evaluation. This includes using Scanning Electron Microscopy (SEM) to examine the microstructure, morphology, and measure the distribution of GO and other constituents within the DNA polymerization gel matrix. This characterization could elucidate synergistic relationships between components and their contributions of the material's components to the material's mechanical properties. Techniques like Dynamic Light Scattering (DLS) could be used to characterize the internal structure, domain formations, and clustering of polymer and GO molecules to study structure formation. Fluorescence microscopy could identify spatial and temporal patterns of DNA uptake or release during swelling or shrinking. Fourier-Transform Infrared Spectroscopy (FTIR) could make it possible to identify interactions between DNA and GO. Moreover, rheological studies should be integral to these future efforts, as the data are crucial for predicting and optimizing the material's performance under real-world conditions, especially when subjected to mechanical stresses.

Aging could also impact the performance of GO-DNA CPGs, especially their swelling/shrinking behavior and stability. Over time, changes in hydrogen bonding within the hydrogel matrix can alter its mechanical properties and affect its ability to absorb and release water. Thes changes can lead to variations in the swelling and shrinking cycles, potentially reducing the reproducibility and reliability of experimental results. Furthermore, the formation of aggregates as the sample ages can compromise the uniform distribution of GO nanosheets within the hydrogel, disrupting the composite's structural integrity and leading to heterogeneous swelling behavior and localized mechanical weaknesses. We plan future studies on characterizing and mitigating aging effects and the stability and performance of the composites over time.

Furthermore, the incorporation of alternative nanomaterials into DNA polymerization gels could enhance multifunctionality. For instance, nanoparticles made of gold (Au) could be exploited for their distinctive optical properties. Including gold nanoparticles may confer unique functionalities, such as localized surface plasmon resonance, which could be harnessed for biosensing applications or even targeted drug delivery. Also, including carbon nanotubes and other 2D layered materials could endow novel electrical properties relevant to hydrogel bioelectronics.

FUNDING

Research reported in this publication was supported by the National Science Foundation EFMA 1830893, EFMA-2318093, and CBET-2348680, Army Research Office W911NF2010057, and Office of Naval Research N00014-23-1-2868.

CONFLICT OF INTEREST STATEMENT

JHU has filed patents on DNA polymerization hydrogels, on which RSh, RSc, and DHG are listed as inventors.

AUTHORS CONTRIBUTIONS

RSh, QH, RSc, and DHG conceptualized the study. RSh conducted the experiments and analyzed the data. RSh wrote the manuscript with edits from QH, RSc, and DHG.

DATA AVAILABILITY STATEMENT

Other than data plotted in the graphs in the paper, no other datasets were generated or analyzed during the current study. An SI document is included.

REFERENCES

- [1] O. Erol, A. Pantula, W. Liu, D. H. Gracias, Adv. Mater. Technol. 2019, 4, 1900043.
- [2] L. Ionov, Mater. Today 2014, 17, 494.
- [3] A. P. Liu, E. A. Appel, P. D. Ashby, B. M. Baker, E. Franco, L. Gu, K. Haynes, N. S. Joshi, A. M. Kloxin, P. H. J. Kouwer, J. Mittal, L. Morsut, V. Noireaux, S. Parekh, R. Schulman, S. K. Y. Tang, M. T. Valentine, S. L. Vega, W. Weber, N. Stephanopoulos, O. Chaudhuri, *Nat. Mater.* 2022, 21, 390.
- [4] F. Li, D. Lyu, S. Liu, W. Guo, Adv. Mater. 2020, 32, 1806538.
- [5] D. Wang, P. Liu, D. Luo, Angew. Chemie Int. Ed. 2022, 61, e202110666.
- [6] D. Wang, Y. Hu, P. Liu, D. Luo, Acc. Chem. Res. 2017, 50, 733.
- [7] F. Li, J. Tang, J. Geng, D. Luo, D. Yang, Prog. Polym. Sci. 2019, 98, 101163.
- [8] A. Cangialosi, C. Yoon, J. Liu, Q. Huang, J. Guo, T. D. Nguyen, D. H. Gracias, R. Schulman, Science 2017, 357, 1126.
- [9] R. Shi, J. Fern, W. Xu, S. Jia, Q. Huang, G. Pahapale, R. Schulman, D. H. Gracias, Small 2020, 16, 2002946.
- [10] R. Shi, K.-L. Chen, J. Fern, S. Deng, Y. Liu, D. Scalise, Q. Huang, N. J. Cowan, D. H. Gracias, R. Schulman, bioRxiv 2022, 2022.09.21.508918.
- [11] D. C. Lin, B. Yurke, N. A. Langrana, J. Mater. Res. 2005, 20, 1456.
- [12] M. Shibayama, T. Tanaka, in Adv. Polym. Sci., 1993, pp. 1-62.

- [13] T. S. Shim, Z. G. Estephan, Z. Qian, J. H. Prosser, S. Y. Lee, D. M. Chenoweth, D. Lee, S. J. Park, J. C. Crocker, Nat. Nanotechnol. 2017, 12, 41.
- [14] A. Pantula, B. Datta, Y. Shi, M. Wang, J. Liu, S. Deng, N. J. Cowan, T. D. Nguyen, D. H. Gracias, Sci. Robot. 2023, 7, eadd2903.
- [15] P. Thoniyot, M. J. Tan, A. A. Karim, D. J. Young, X. J. Loh, Adv. Sci. 2015, 2, 1.
- [16] A. Sydney Gladman, E. A. Matsumoto, R. G. Nuzzo, L. Mahadevan, J. A. Lewis, *Nat. Mater.* 2016, 15, 413.
- [17] Z. Zhao, X. Kuang, C. Yuan, H. J. Qi, D. Fang, ACS Appl. Mater. Interfaces 2018, 10, 19932.
- [18] S. K. Pal, A. Agarwal, N. L. Abbott, Small 2009, 5, 2589.
- [19] T.-S. Jang, H.-D. Jung, H. M. Pan, W. T. Han, S. Chen, J. Song, Int. J. bioprinting 2018, 4, 126.
- [20] J. Chen, K. Park, J. Control. Release 2000, 65, 73.
- [21] K. Kabiri, H. Omidian, M. J. Zohuriaan-Mehr, S. Doroudiani, *Polym. Compos.* 2011, 32, 277.
- [22] H. Lu, S. Zhang, L. Guo, W. Li, RSC Adv. 2017, 7, 51008.
- [23] S. Bashir, K. Hasan, M. Hina, R. A. Soomro, M. A. Mujtaba, S. Ramesh, K. Ramesh, N. Duraisamy, R. Manikam, J. Electroanal. Chem. 2021, 898, 115626.
- [24] G. Nassar, E. Daou, R. Najjar, M. Bassil, R. Habchi, Carbon Trends 2021, 4, 100065.
- [25] W. Xu, K. S. Kwok, D. H. Gracias, Acc. Chem. Res. **2018**, *51*, 436.
- [26] Y. Zou, R. Liu, W. Zhong, W. Yang, J. Mater. Chem. A 2018, 6, 8568.
- [27] A. Xavier Mendes, S. Moraes Silva, C. D. O'Connell, S. Duchi, A. F. Quigley, R. M. I. Kapsa, S. E. Moulton, ACS Biomater. Sci. Eng. 2021, 7, 2279.
- [28] A. Marrella, A. Lagazzo, F. Barberis, T. Catelani, R. Quarto, S. Scaglione, Carbon N. Y. 2017, 115, 608.
- [29] C. Pan, L. Liu, Q. Chen, Q. Zhang, G. Guo, ACS Appl. Mater. Interfaces 2017, 9, 38052.



Supplementary Information (SI) for

Ultra-Thin Graphene Oxide (GO)-DNA Composite Polymerization Gels (CPGs)

Ruohong Shi¹, Qi Huang¹, Rebecca Schulman¹⁻⁴*, and David H. Gracias^{1, 3-8}*

¹Department of Chemical and Biomolecular Engineering, Johns Hopkins University, Baltimore, MD. USA.

²Department of Computer Science, Johns Hopkins University, Baltimore, MD, USA.

³Laboratory for Computational Sensing and Robotics (LCSR), Johns Hopkins University, Baltimore, MD, USA.

⁴Department of Chemistry, Johns Hopkins University, Baltimore, MD, USA.

⁵Center for MicroPhysiological Systems (MPS), Johns Hopkins University, Baltimore, MD, USA.

⁶Department of Oncology, Johns Hopkins School of Medicine, Baltimore, MD, USA.

⁷Sidney Kimmel Comprehensive Cancer Center (SKCCC), Johns Hopkins School of Medicine, Baltimore, MD, USA.

⁸Department of Materials Science and Engineering, Johns Hopkins University, Baltimore, MD, USA.

*Corresponding authors: dgracias@jhu.edu; rschulman@jhu.edu

SUPPLEMENTARY FIGURES

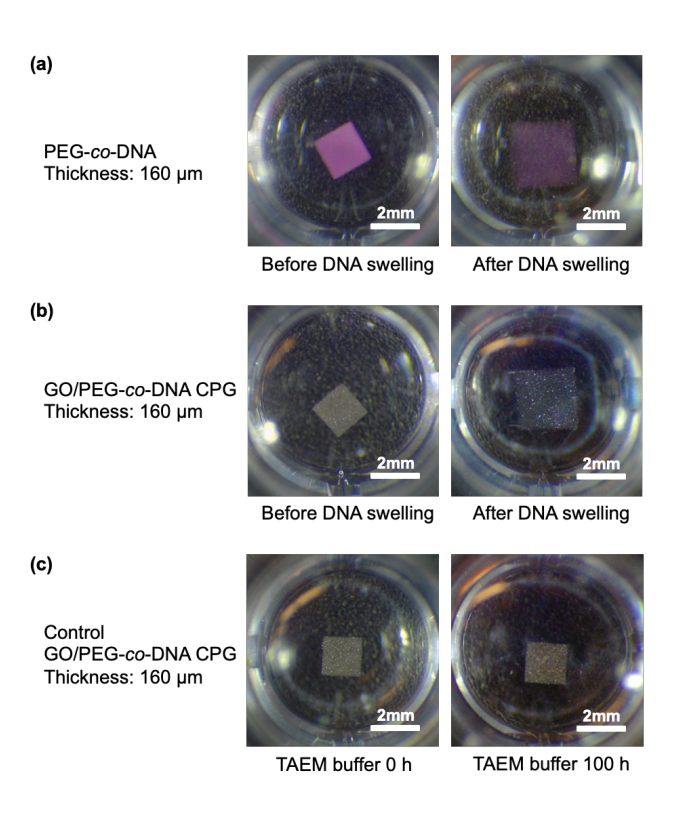


Figure S1 | Bright-field images of GO-DNA CPGs. (a) A PEG-co-DNA gel (no GO, with a fluorescent dye, 160 μ m thick) before and after 100 hours of DNA growth activator-directed swelling. (b) A GO/PEG-co-DNA CPG (without fluorescent dye, 160 μ m thick) before and after 100 hours of DNA growth activator-directed swelling. (c) A GO/PEG-co-DNA CPG (without fluorescent dye, 160 μ m thick) before and after 100 hours of soaking in 1×TAEM buffer.

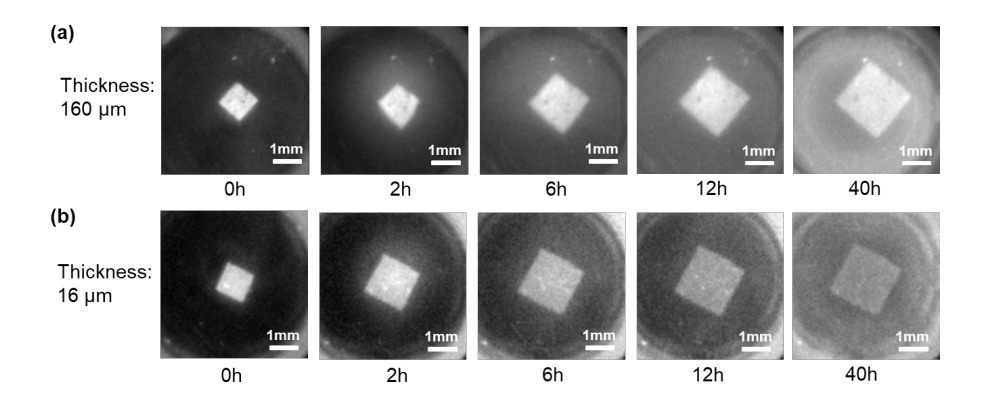


Figure S2 | Fluorescent micrographs of GO/PAAM-co-BIS-DNA CPGs with varying thicknesses of, (a)160 μ m, and (b)16 μ m swelling using DNA growth activators.

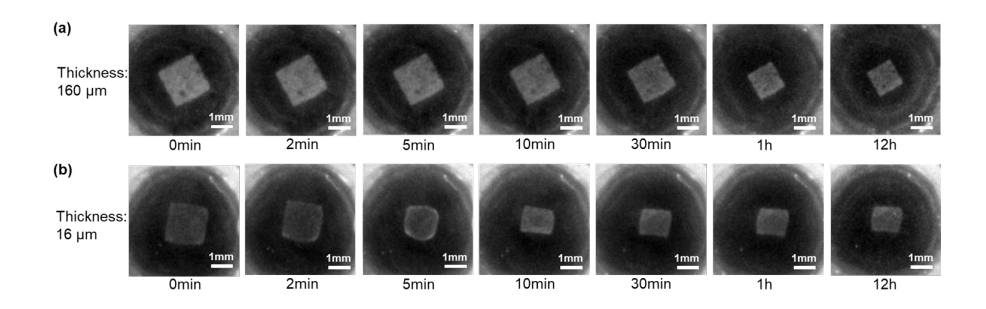


Figure S3 | Fluorescent micrographs of GO/PAAM-co-BIS-DNA gels with varying thicknesses of, (a)160 μ m, and (b)16 μ m shrinking using DNA shrinking activators.

MATERIALS & METHODS

Materials and DNA

Polyethylene glycol diacrylate Mn 10,000 (PEGDA10k) was obtained from Sigma-Aldrich (Cat. No. 729094). The fluorophore RhodamineB-methacrylate was purchased from PolySciences, Inc. (Cat. No. 25404-100) and was used to visualize the hydrogels. Acrylamide (Bio-Rad, Cat. No. 161-0100) and N, N'-methylenebis(acrylamide) (Sigma-Aldrich, #146072) were solubilized in MilliQ purified water for a 40 wt% stock and a 100 mM stock, respectively. The UV-sensitive initiator Omnirad 2100 (iGM Resins USA, #55924582) photoinitiator was used to polymerize hydrogels. Single-layer graphene oxide (H method) was obtained from ACS Material (Product No. GNOP1001) and was dispersed in MilliQ purified water for a 20 wt% stock. All DNA strands were purchased with standard desalting purification from Integrated DNA Technologies, Inc. Acrydite-modified strands were solubilized using 1× TAE buffer (Life Technologies, Cat. No. 24710-030) supplemented with 12.5 mM magnesium acetate tetrahydrate (Sigma-Aldrich, Cat. No. M5661).

All unmodified DNA strands were solubilized using MilliQ purified water. DNA sequences are listed in Table 1. DNA crosslink complexes were annealed in $1\times$ TAE buffer supplemented with 12.5 mM magnesium acetate tetrahydrate (TAEM) from 90 to 20 °C in an Eppendorf PCR at 1 °C/minute at 3 mM per strand. Growth activator strands were heated to 95 °C for 15 minutes at a concentration of 400 μ M in MilliQ purified water, followed by flash cooling on ice for 3 minutes. Shrinking activator strands were made to a 400 μ M stock in MilliQ purified water.

Preparation of DNA pre-gel solution

The concentrations of the components in GO/PAAM-co-BIS-DNA pre-gel solution were: 1× TAEM, 1.41 M of acrylamide (BIO-RAD #161-0100), 5 mM of N, N'-methylenebis(acrylamide), 1.154 mM DNA crosslinks, 2%v/v Omnirad 2100, 2.74 mM methacryloxyethyl thiocarbamoyl rhodamine B (Polysciences, Inc., #23591) (as needed), and 4 wt% GO. The concentrations of the components in the GO/PEG-co-DNA pre-gel solution were the same as those in the GO/PAAM-co-BIS-DNA pre-gel solution except PEGDA-MW10k (Sigma-Aldrich, #729094) was 10wt%, and was used in place of acrylamide and bis-acrylamide.

PEGDA10k powder (or acrylamide and N, N'-methylenebis(acrylamide) stock solution) was mixed with MilliQ purified water and 10× TAEM. After the PEGDA10k was fully dissolved, Acrydite-modified DNA, RhodamineB-methacrylate, and Omnirad 2100 (75% v/v in butanol) were mixed into the solution. GO stock was sonicated for 1 minute and then added to the pre-gel solution. After mixing with a pipette, the pre-gel solution was sonicated for 5 minutes and degassed for 15 minutes.

Photopatterning process for GO-DNA CPGs

We assembled photolithography chambers, as reported previously. $^{[11,12,33]}$ To photo pattern square-shaped DNA hydrogels, we designed masks with 1mm side-length squares using AutoCAD and made the Cr masks. The thickness of the patterned hydrogel could be tuned using different thicknesses of spacers. The spacer materials include paper tape, aluminum foil with 160 μm and 16 μm thicknesses, and custom-made 8 μm thick SU-8 spacers on glass substrates. The pre-gel solution was injected into the photo patterning chamber and then exposed to a 365 nm UV light source (Neutronix Quintel aligner) with

an energy dose of 160 mJ/cm² for GO/PAAM-co-BIS-DNA gels or 600 mJ/cm² for GO/PEG-co-DNA gels. The chamber was gently disassembled after the polymerization. We use TAEM to wash the extra pre-gel solution and hydrate the gel. The hydrogel was stored in TAEM at 4°C to achieve complete hydration until use within 2 weeks. The intrinsic swelling in TAEM was not included in the swelling kinetics calculations.

Synthesis of 8 µm thick SU-8 spacers on glass substrates

We utilized SU-8 to make 8 μ m thick spacers on glass slides. We spin-coated SU-8 2005 with 1000 rpm. After spin-coating, we bake the film on hotplates at 65 °C for 1 minute, then at 95 °C for 3 minutes, and at 65 °C for another minute. Then, we exposed the SU-8 using 120 mJ/cm² of 365 nm UV light. A square photomask was used to define the shape of the spacer. After exposure, we repeated the baking process as a post-baking process. Then, the film was developed in SU-8 developer for 1 minute. We rinsed the SU-8 film with isopropyl alcohol after developing it to prepare it for use.

Swelling characterization of GO-DNA GPG

Hydrogel swelling experiments were conducted with one hydrogel per well in 96well plates (Fisher Scientific). Solution composition and solute concentrations are as stated below: gels were expanded in TAEM supplemented with 0.01%v/v Tween20 (Sigma, #051M01811V) (TAEM-Tween20) to prevent gels from sticking to the well surfaces. 150 μL of TAEM-Tween20 solution containing 60 μM DNA growth activators (99% polymerizing, 1% terminating) was added to each well. After 35-70 hours of swelling, the DNA solution was switched to 100 μ L TAEM-Tween20 for 15 mins, and the solution was removed, and then 150 µL TAEM-Tween20 shrinking activators solution was added. Images were captured every 30 minutes (swelling), or every 1 minute in the first hour and every 15 minutes after the first hour (shrinking), using a humidified Syngene G: Box EF2 gel imager equipped with a blue light transilluminator (Clare Chemical, Em. max ~450 nm) and a UV032 filter (Syngene, bandpass 572-630 nm). The relative change in the side length of the hydrogels was measured using MATLAB. The edge of the hydrogel was determined using standard intensity-based thresholding and mask image analysis, as stated in previous studies. Bright-field images were taken using a Hayear 4K Microscope Camera (HY-1070).

Table S1

DNA sequences. All strands were ordered from IDT in their lyophilized form, resuspended with TAEM solution, and stored at -20 $^{\circ}$ C until use. /5ACryd/ indicates an Acrydite modification.

Name	Sequence
Acrydite-	/5ACryd/CTATCTATCCATCACCCTCACCTTAC
modified DNA	
crosslink_A	
Acrydite-	/5ACryd/GGTGTAAGGTGAGGGTGATGGTAA
modified DNA	
crosslink_R	
Growth	TTACCATCACCTCACCTTACTTGTAGATTTTTTGTAAG
activator 1	GTGAGGGTGATGGATAGATAGGGTAGGTGAATGGGA
Growth	TTACCATCACCTCACCTTACCTCTCCACTTTTTGTAAG
terminator 1	GTGAGGGTGATGGATAGATAGGGTAGGTGAATGGGA
Growth	TATGAGTGAGTTAGGATCTACAAGTAAGGTGAGGGTGA
activator 2	TGGTTTTCTATCTATCCATCACCCTCACCTTACACC
Growth	TATGAGTGAGTTAGGATCTACAAGTAAGGTGAGGGTGA
terminator 2	TGGTTTTTACGAGCCTCCATCACCCTCACCTTACACC
Shrinking	TCCCATTCACCTACCATAGATAGCCATCACCCTCACCTT
activator 1	AC
Shrinking	CCATCACCTCACCTTACTTGTAGATCCTAACTCACTCA
activator 2	TA